

UNIVERSIDAD DE LOS ANDES

THESIS

---

# Two-Photon Imaging Using Tunable Spatial Correlations

---

*Author:*

Juan VARGAS

*Supervisor:*

Dr. Alejandra  
VALENCIA

*A thesis submitted in fulfillment of the requirements  
for the degree of Physicist*

*in the*

Quantum Optics  
Physics Department



May 8, 2018

# Declaration of Authorship

I, Juan VARGAS, declare that this thesis titled, "Two-Photon Imaging Using Tunable Spatial Correlations" and the work presented in it are my own. I confirm that:

- This work was done wholly or mainly while in candidature for a research degree at this University.
- Where any part of this thesis has previously been submitted for a degree or any other qualification at this University or any other institution, this has been clearly stated.
- Where I have consulted the published work of others, this is always clearly attributed.
- Where I have quoted from the work of others, the source is always given. With the exception of such quotations, this thesis is entirely my own work.
- I have acknowledged all main sources of help.
- Where the thesis is based on work done by myself jointly with others, I have made clear exactly what was done by others and what I have contributed myself.

Signed:

---

Date:

---

*“Nonesenses... later due”*

N.N

UNIVERSIDAD DE LOS ANDES

*Abstract*

Science Faculty  
Physics Department

Physicist

**Two-Photon Imaging Using Tunable Spatial Correlations**

by Juan VARGAS

Two-Photon Imaging is a well studied phenomena, where we take advantage of the different correlations in which the light can be related to reconstruct the image of certain objects. In this Thesis use different spatial correlations of a SPDC light source, where we change these correlations changing the pump waist.

## *Acknowledgements*

The acknowledgments and the people to thank go here, don't forget to include your project advisor...s

# Contents

<b>Declaration of Authorship</b>	<b>i</b>
<b>Abstract</b>	<b>iii</b>
<b>Acknowledgements</b>	<b>iv</b>
<b>1 Introduction</b>	<b>1</b>
<b>2 Theory</b>	<b>5</b>
2.1 Correlations between two photons . . . . .	5
2.1.1 SPDC . . . . .	6
2.1.1.1 Phase matching conditions . . . . .	7
2.1.2 Spatial Correlations . . . . .	8
2.1.3 Tunable Spatial Correlation SPDC source light . . . . .	11
2.2 Imaging . . . . .	11
2.2.1 Standar Imaging . . . . .	12
2.2.2 Two-photon Imaging . . . . .	13
2.2.2.1 Two-photon Imaging using entangled photon	14
2.2.2.2 Propagation of light through 2-f system . . .	15
2.2.2.3 Two-photon Imaging Using Chaotic Sources .	18
<b>3 Experimental Setup</b>	<b>21</b>
3.1 SPDC Setup . . . . .	21
3.1.1 Diode Laser . . . . .	21
3.1.2 Mirror . . . . .	21
3.1.3 Spatial Filter . . . . .	21
3.1.4 Waist Lens . . . . .	24
3.1.5 BBO(Beta Barium Borate) Crystal . . . . .	24
3.2 Spatial Correlations Measurement Setup . . . . .	25
3.2.1 Lens (Fourier Plane) . . . . .	25
3.2.2 Polariser . . . . .	25
3.2.3 Interferometer Filter . . . . .	26
3.2.4 Pin Hole(Arduino) . . . . .	26

3.2.5	Single Photon Counting Module(SPCM)	26
3.2.6	Field-programmable gate array(FPGA)	26
3.2.7	Computer(Data Analysis)	27
3.3	Two-Photon Imaging Setup	27
3.3.1	Mask	27
3.3.2	Folding Mirror	27
3.3.3	Bucket Detector	27
<b>4</b>	<b>Results</b>	<b>29</b>
4.1	Achiving a Gaussian Beam	29
4.2	Finding The Correlated Photons	29
4.3	Experimental Correlations	29
4.3.1	$w_p = ?$	30
4.4	Mask Alignment	30
4.5	Two-Photon Images	31
4.5.1	mask1	31
4.5.2	mask2	31
4.5.3	mask3	31
<b>5</b>	<b>Discussions and Conclusion</b>	<b>32</b>
<b>Bibliography</b>		<b>33</b>

# List of Figures

1.1	Eye seen as a Optical System . . . . .	1
1.2	Two-photon imaging techniche setup . . . . .	2
2.1	Simple Experimental setup for the type-II noncollinear SPDC process . . . . .	6
2.2	Experimental Spatial correlations between a pair of down-converted photons. Right image shows the correlation in the x variable. Left shows the correlation in the y variable, Beam propagating in the z direction . . . . .	9
2.3	Positive(right) and Negative(left) ideal spatial correlations . .	10
2.4	Optical imaging: a lens produces an image on an object at $S_i$ . This distance is defined by the Gaussian thin-lens equation . .	12
2.5	Simple schematic for the Two-photon Imaging . . . . .	13
2.6	Schematic of the first "two-photon imaging" experimental setup, used by Pittman[1] . . . . .	15
2.7	Simple schematic for a Two-photon Imaging using entangled photons and a 2-f system . . . . .	16
2.8	Experimental setup for the Two-photon imaging using thermal light, taken from [2] . . . . .	19
3.1	Experimental Setup for the SPDC light Source . . . . .	21
3.2	Image of the Diode Laser and it's control module, Taken from [3] . . . . .	22
3.3	Mirror and the cavity mount . . . . .	22
3.4	The spatial intensity profile before and after the spatial filtering process , Taken from [4] . . . . .	23
3.5	Basic elements of a Spatial Filter. In our experiment we use a Aspheric Lens of $f = 30mm$ (LA1805-A), a pinhole of $50\mu m$ and a collimating lens of $f = 60mm$ (LA1134-A). Taken from [4]	23
3.6	This helps to form circular apertures of variable radius . . . .	24
3.7	Lens' effect on a Gaussian beam . . . . .	24
3.8	Actual BBO crystal used in experiment . . . . .	25

3.9	Experimental Setup for Obtaining the spatial correlations of a pair of down-converted photons . . . . .	25
3.10	Single Photon Counting Module . . . . .	26
3.11	Experimental Setup for the Two-photon Imaging . . . . .	27
3.12	Foldind Mirror, it is in the position for measuring the correlations . . . . .	28
4.1	We are moving the translational translational stage, to locate the spot where the correlated photon are, for this try me moved the <i>y</i> direction . . . . .	29
4.2	Localization of the mask with an square . . . . .	30
4.3	Moving the L Mask in order to put it in the most central spot . . . . .	30
4.4	Long exposure of the definitive localization of the mask, in this try we leave the detector in each place for 30 seconds, we also make the steps of the detector smaller, 0.1mm . . . . .	31
4.5	Localization of the mask with an square . . . . .	31

*For/Dedicated to/To my...*

# Chapter 1

## Introduction

Imaging is a process that we are doing all time, we have a pair of optical systems (OS) that are mapping constantly, and doing a recreation of the things around us. This pair of OS is what we call eyes, without them we would be able just to *feel* what surround us, it would be impossible to *see*, to do an *image* of our surroundings. The components of the eye are a well established optical system, this OS uses the light that is reflected or scattered from the objects and then comes towards the eye. At the back of the eye we have a photodetector that is called Retina, it converts the photons into electrical signals that travels through our Brain, where the image is then recovered. Figure ?? show a really simplified schematics of the eye seen as an OS.

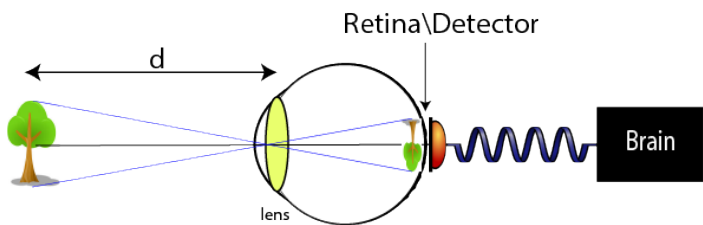


FIGURE 1.1: Eye seen as a Optical System

For taking a photograph of an object, traditionally, we need to face a camera detector (CCD) to the object, in a similar way we have to point our eyes to the objects we are seeing, Figure ?? . Both retina and CCD saves some kind of the spatial shape of the light that comes through. This spatial information is necessary then for the process of reconstructing an image of an object, from this statement we can start talking about a spot-to-spot correspondence between the object and the image plane. It is important to point out that we usually make images, 2D representations, of 3D objects. For this reason we talk about an image plane, which is the plane where, depending on the OS, the 2D representation of the object is going to be formed.

What would happen if our retina or CCD stoped saving this spatial references?, if our retina now is only able to detect that light is going through, not

where. It is clear that in this situation the imaging process would be impossible, without any spatial information is not possible to create a representation in 2D of something.

Two-photon imaging is technique that could solve this dilemma. It is also a optical imaging experiment that started to draw attention after Pittman's first realisation [1]. As the name suggest it, Two-photon imaging, we use a second photon to reconstruct the image. In other words, in order to reconstruct an image we use two detectors that are spatially separated. In this opportunity we use a detector that is toward the light source  $D_A$  and another detector  $D_B$  that is towards the object. In Figure 1.2 there is schematic of the situation, we collect the light from the source and after the object, in this case a double slit. Where  $D_B$  is a big detector that collects all the light after the object, while  $D_A$  is a small detector that is capable of scanning the transverse direction of the light propagation.

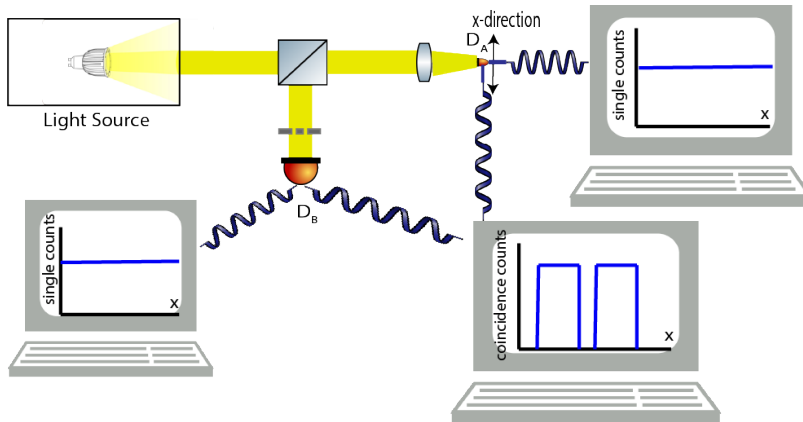


FIGURE 1.2: Two-photon imaging technique setup

There are different types of Two-photon imaging, and they differs from each other in the nature of the light source used. The first two-photon imaging realisation used entangled photon pairs as the light source. In 1995 Pittman, realized a quantum two-photon geometric optical effect. They have successfully performed optical imaging by means of a quantum-mechanical entangled source[1].

The second kind of imaging uses chaotic light. This light can be understood as the radiation coming from a blackbody at thermal equilibrium in temperature, it means the light source is composed by a huge number of photons and they are randomly distributed in the possible momentum and frequencies. this is because each photon corresponds to a transition in one of the trilion atoms or molecules of the light source. Valencia *et al.* where

the first ones to present a experimental demonstration of two-photon ghost imaging with thermal-like sources[2].

It is possible to reconstruct the image in this two experiments because there is some kind of correlation between the photon that are generated from the source, in the quantum light source, there is entanglement between the pair of used photons. Depending in certains situations we can say the pair is anti-correlated[5]. In the experiment of the chaotic light, the source is modeled as an incoherent statistical mixture of many pairs of photons; the various two-photon probability amplitudes are provided by the entire ensemble of photon pairs. There is a correlation between this probability amplitudes that allows to retrive the image.

In our experiment we have done a Two-photon imaging using a source of entangled photons, we are able to change the how the generated photons are entangled, more specifically, we can tune the way the transverse momentums  $\vec{q}_A$  and  $\vec{q}_B$  are correlated. Changing the shape of this spatial correlation will have an effect in the obtained image. The pair of photons are created by focusing a laser beam to a nonlinear crystal, this process is named SPDC. We control the shape of the spatial correlations by changing the pump waist of the laser. This monograph intend to describe this experiment and develop the theory behind it, also show some hits about the possible effects of the different spatial correlations in the image.

As pointed out before, this experiment consist in a source light and two arms, one that interacts with an object, path  $B$ , and another that propagates through free space, path  $A$ . So this last one can be simulated by a computer using Fresnel's propagation theory, doing so is called the Computational Two-photon Imaging. It allows us to simulate the electric field data, to be obtain it before, during or after the data from the reflected arm is generated ( $B$ ),eliminating the need for collecting the data generated in the transmitted path ( $A$ ). Also we have to use less opto-electronical elements on the optical table, simplifying the original setup and reducing considerably the amount of data generated. The resulting detection module consist only in one detector, a bucket detector that collects a single pixel (no spatial information) on light which has been transmitted through or reflected from the object. In this situation only one light beam and one photodetector are required, this means that this imaging configuration cannot depend on non-local two-photon interference[6].

This document is organized as follows: Chapter 2 presents a theoretical discusion about the fundamental aspects of the two-photon imaging, with an

especial focus on the SPDC generation of entangled photons, and the imaging using this pairs as the source light. In chapter 3 there is a meticulous explanation of the experimental setups used in this monograph, explaining each element used in the optical table. The experimental results are presented in the chapter 4. The conclusions and further discussion are on chapter 5.

# Chapter 2

## Theory

In Here we will discuss some important facts to get a complete understanding in the physical phenomena that is happening. Specially we will develop the notions that are crucial in the understanding of the Two-photon imaging using entangled light, been this said we will start talking about correlations.

### 2.1 Correlations between two photons

The term "correlation" is crucial at this point, and it refers to the relation of two or more situations have. For example we can establish a correlations between the US dollar currency exchange rate and the prices of technology in one country. These two things have direct relation, if one blows up, the other one will too. These two situations, or variables, can have a strong correlations or a week one.

Indeed in quantum physics we can have a pair of photons that are so strongly correlated, in their possible variables (spatial and temporal), that we say they are entangled. This statement can leads us to a dense discussion about the nature of this entanglement, a discussion that were started between Einstein and Bohr in the first years of quantum physics [7].

To avoid this discussion we will just talk about correlations, and when referring about a pair of correlated photons, we will mean that this pair of photons are correlated in one or varius of their variables. They can be correlated in momentum, meaning that when one photon have a given  $\vec{q}_i$  momentum and the other photon have a  $\vec{q}_j$  momentum that is determined by the first, this relations is the momentum correlations a we can work out an expression for this relationship.

### 2.1.1 SPDC

As the title of this work implies, we need a source light that produces pair of photons, and we would like to exploit the advantages of strong correlations between them. The photons generated via spontaneous parametric down conversion (SPDC) are widely used in quantum optics experiments. The popularity of this source of paired photons is strongly related to the relative simplicity of its experimental realisation, and to the variety of quantum features that down converted photons can exhibit. The generated photons via SPDC can be correlated in different degrees of freedom, for example in polarisation, in frequency and in the equivalent degrees of freedom: 'orbital angular momentum, space and transverse momentum [8].

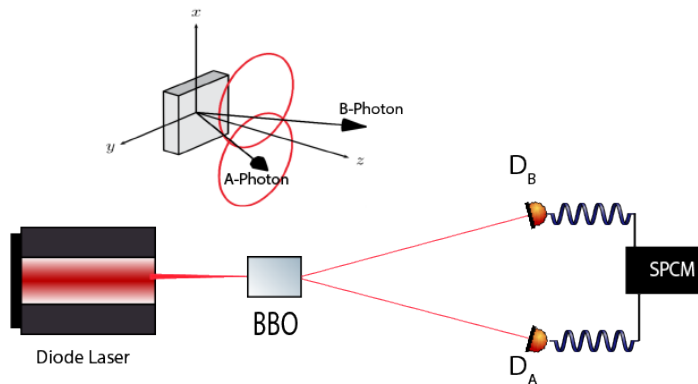


FIGURE 2.1: Simple Experimental setup for the type-II non-collinear SPDC process

SPDC is an optical process in which focus a beam pump, that is propagating in the  $z$ -direction, to a nonlinear crystal of length  $L$ . Depending of the polarisation direction of the produced photons, the nonlinear crystals can be classified in types. The type-0 crystal will produce pairs that are polarised in the source light direction. The type-I will do the proper, but this time the polarisation will be in the perpendicular direction of the pump. The last type, type-two crystal will produce a pair of photons, one with the polarisation in the same direction as the pump, and the other one perpendicular. The generated pair can emerge from the crystal in a collinearly or noncollinearly.

Using first order perturbation and the paraxial approximation, the two-photon state is given by:

$$|\Psi\rangle = \int dq_B dq_A d\Omega_B d\Omega_A \times [\Phi(q_B, \Omega_B; q_A, \Omega_A) \hat{a}^\dagger(\Omega_B, q_B) \hat{a}^\dagger(\Omega_A, q_A) + \Phi(q_A, \Omega_A; q_B, \Omega_B) \hat{a}^\dagger(\Omega_B, q_B) \hat{a}^\dagger(\Omega_A, q_A)] \quad (2.1)$$

Where this state function depends on the transverse wave vectors  $q_n = (q_n^x, q_n^y)$  and frequency detuning,  $\Omega_n = \omega_n - \omega_0^n$ , around the central frequencies,  $\omega_0^n$ , for the photon at the path  $A$  or  $B$  ( $n = A, B$ ). The  $\Phi(q_B, \Omega_B; q_A, \Omega_A)$  and  $\Phi(q_A, \Omega_A; q_B, \Omega_B)$  are the mode functions or biphotons that contains all the informations about the correlations between the pair of down-converted photons. The operator  $\hat{a}^\dagger$  indicates the creations of an  $n$ -polarized photon with transverse momentum  $q_n$ , and frequency detuning  $\Omega_n$  [9].

In the optical table we put a polariser at certain directions at the detections modules, filtering some of the photons before reaching the detector, this filtering also have a mathematical effect in our model, it is possible now to write 2.1 different, dropping one term:

$$|\Psi\rangle = \int dq_B dq_A d\Omega_B d\Omega_A \times [\Phi(q_B, \Omega_B; q_A, \Omega_A) \hat{a}^\dagger(\Omega_B, q_B) \hat{a}^\dagger(\Omega_A, q_A)] |0\rangle \quad (2.2)$$

The mode function  $\Phi(q_B, \Omega_B; q_A, \Omega_A)$  is related with the joint probability of detecting both an  $B$ -polarized photon, with tranverse momentum  $q_B$  and frequency detuning  $\Omega_B$ , at the detector  $B$  and an  $A$ -polarized photon, with tranverse momentum  $q_A$  and frequency detuning  $\Omega_A$ , at the detector  $A$ .

### 2.1.1.1 Phase matching conditions

In particular,  $\Phi(q_B, \Omega_B; q_A, \Omega_A)$  reads [8]:

$$\Phi(q_B, \Omega_B; q_A, \Omega_A) = \mathcal{N} \alpha(\Delta_0, \Delta_1) \beta(\Omega_B, \Omega_A) \times \text{sinc}\left(\frac{\Delta_k L}{2}\right) e^{i\frac{\Delta_k L}{2}} \quad (2.3)$$

Where  $\mathcal{N}$  is a normalisation constant,  $\alpha(\Delta_0, \Delta_1)$  and  $\beta(\Omega_B, \Omega_A)$  yields the informations of the pump's transverse and spectral distribution, respectively,  $L$  is the length of the nonlinear crystal. For the process that is happening inside the crystal, there are some conditions that have to be fulfilled. These conditions are related with the energy and momentum conservations inside the parametric down conversion process. The terms  $\Delta_0$ ,  $\Delta_1$  and  $\Delta_k$  are functions that result from the phase matching conditions and read:

$$\Delta_0 = q_B^x + q_A^x \quad (2.4)$$

$$\Delta_1 = q_A^y \cos\phi_A + q_B^y \cos\phi_B - N_B \Omega_B \sin\phi_B + N_A \Omega_A \sin\phi_A - \rho_B q_B^x \sin\phi_B \quad (2.5)$$

$$\Delta_k = N_p(\Omega_B + \Omega_A) - N_B \Omega_B \cos\phi_B - N_A \Omega_A \cos\phi_A - q_B^y \sin\Omega_B + q_A^y \sin\Omega_A + \rho_p \Delta_0 - \rho_B q_B^x \cos\phi_B \quad (2.6)$$

The angles  $\phi_B$  and  $\phi_A$  are the creation angles of the down-converted photons inside the crystal with respect to the pump's propagation direction, whereas the angles  $\rho_p$  and  $\rho_B$  account for the walk-off of the pump  $p$  and the  $B$  down-converted photon, respectively. In this study,  $\phi_B$  and  $\phi_A$  are treated as constants, mainly because the scanned transverse momentum regions represent a small portion around the emission angles.  $N_n$  denotes the inverse of the group velocity for each photon.

### 2.1.2 Spatial Correlations

In order to observe the correlations presented in 2.3 we have to take into account some considerations about the description of the things we have in optical table. First of all we have a pump beam with a Gaussian profile with waist  $w_p$  in such way that  $\alpha(\Delta_0, \Delta_1) \propto \exp[-w_p^2(\Delta_0^2 + \Delta_1^2)/4]$ , a CW pump laser, mathematically represented by  $\beta(\Omega_B, \Omega_A) \propto \delta(\Omega_B + \Omega_A)$ . Making the approximations for the sinc function by a Gaussian functions with the same width at  $1/e^2$  of its maximum, i.e.,  $\text{sinc}(x) \approx \exp(-\gamma x^2)$  with  $\gamma$  equal 0.193. The mode function reduces to:

$$\Phi(q_B, \Omega_B; q_A, \Omega_A) = \mathcal{N} \beta(\Omega_B, \Omega_A) \times \exp \left[ -\frac{w_p^2(\Delta_0^2 + \Delta_1^2)}{4} - \gamma \left( \frac{\Delta_k L}{2} \right)^2 + i \frac{\Delta_k L}{2} \right] \quad (2.7)$$

In order to observe the transverse correlations (spatial correlations), the frequency information has to be traced out, in the optical table this can be achieved by placing some interferometer filters before detection. This spectral filters are modeled as  $f_n(\Omega_n) = \exp[-\Omega_n^2/(4\sigma_n^2)]$ , with bandwidth  $\sigma_n$  chosen to achieve a regimen where the spatial-spectral correlations are completely broken [5]. To achieve this mathematically we have to integrate 2.7 around the spatial variables:

$$\tilde{\Phi}(q_B, q_A) = \int d\Omega_B d\Omega_A f_B(\Omega_B) f_A(\Omega_A) \Phi(q_B, \Omega_B; q_A, \Omega_A) \quad (2.8)$$

Figure 2.2 show a couple of examples of how these correlations we are talking about look like. These correlations have some kind of circular shape, and show how strong is the possibility of detecting a photon at a given position, looking at the first graph, there is a great chance of detecting simultaneously a photon at  $x_B = 0$  and at  $x_A = 0$ . Now if we look at the left graph, it is showing the correlation of the pair of photons in the  $y$  direction, there is

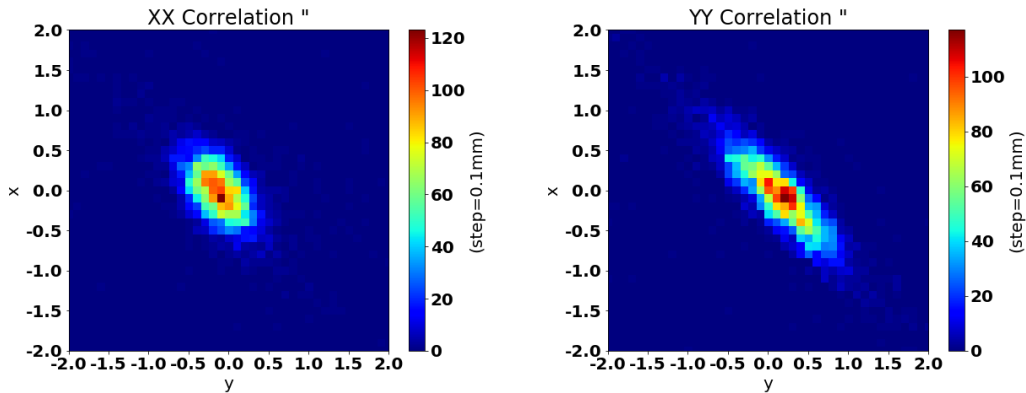


FIGURE 2.2: Experimental Spatial correlations between a pair of down-converted photons. Right image shows the correlation in the  $x$  variable. Left shows the correlation in the  $y$  variable  
Beam propagating in the  $z$  direction

a significant probability of measuring simultaneously a photon at  $y_B = 0.4$  and at  $y_A = -0.4$ . It is interesting how in this case there is a "negative" correlation, the expected position at which we will find the other photon, is at the same, but negative position. Another interesting fact we have to point out, is that this correlations algo can be sharper, the  $x$  correlation have a more circular shape, making wider the possible values for a given  $x_B$ . In contrast the  $y$  correlation is more eliptic, meaning it restring the possible values por a given  $y_B$ . It is easy to think how a strong correlation should look like, a strong correlations in spatial variables would mean that if we have the position of one photon at the position  $x_B$  we immediately would know which  $x_A$  have the other photon, this king of ideal spatial correlation would look like a straigth line really thin, Figure 2.3.

The Biphoton then takes a quadratic form[8]:

$$\tilde{\Phi}(q_B, q_A) = N \exp \left[ -\frac{1}{2} x^T A x + i b^T x \right] \quad (2.9)$$

where  $N$  is a normalization constant, that satisfies  $\int \int |\tilde{\Phi}(q_B, q_A)|^2 d^2 q_B d^2 q_A = 1$ .  $x$  is a 4-dimensional vector defined as  $x = (q_B^x, q_B^y, q_A^x, q_A^y)$ ,  $A$  is a  $4 \times 4$  real-valued, symmetric, positive definite matrix and  $b$  is a 4-dimensional vector.  $A$  and  $b$  are defined from the phase-matching conditions of the SPDC process.  $x^T$  and  $b^T$  denote the transpose of  $x$  and  $b$ .  $A$  and  $b$  are functions that depend of all the relevant parameters in the experiment such as the length of the crystal  $L$ , pump waist  $w_p$ , creation angles inside the crystal  $\varphi_n$  and the width of the spectral filter  $\sigma_n$ .

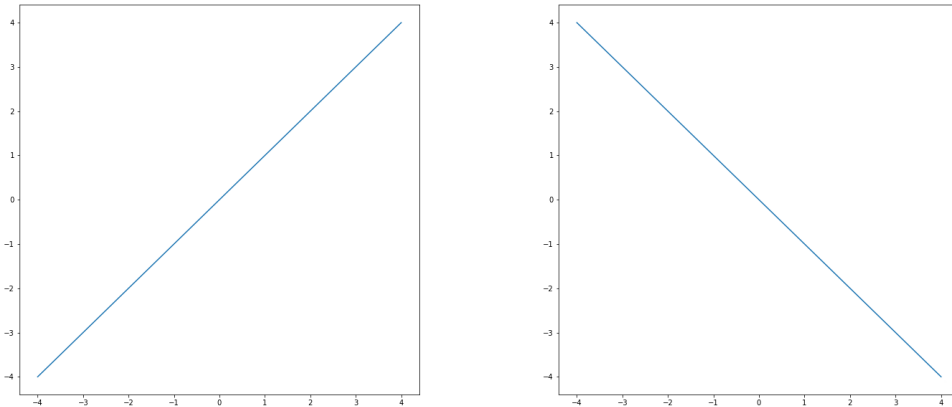


FIGURE 2.3: Positive(right) and Negative(left) ideal spatial correlations

To have a general numerical approach to  $\tilde{\Phi}(\vec{q}_B, \vec{q}_A)$ , it is desired to write it as generic correlations instead of the experimental parameters. This can be done by noticing that the amplitude of  $\tilde{\Phi}(\vec{q}_B, \vec{q}_A)$  has the form of a 4-dimensional gaussian distribution, given by

$$f(x) = \tilde{N} e^{-\frac{1}{2}x^T \Sigma^{-1} x}, \quad (2.10)$$

where  $\tilde{N}$  is a normalization constant satisfying  $\int f(x) d^4x = 1$ ,  $\Sigma^{-1}$  is the inverse of the covariance matrix that contains the correlations between the different elements of  $x$ . With  $x_i$   $i = 0, 1, 2, 3$ ,  $\Sigma$  can be written as:

$$\Sigma_{ij} = \sigma_{x_i} \sigma_{x_j} \rho_{x_i x_j} \quad (2.11)$$

where  $\sigma_i$  denotes the square root of the variance of  $x_i$  and  $\rho_{x_i x_j}$  denotes the Pearson correlation coefficient between  $x_i$  and  $x_j$ . This coefficient quantifies how strong is the linear correlation between  $x_i$  and  $x_j$ [10]. By using Eq.(2.11), the correlations between the spatial variables of the photons can be manually modified in Eq.(2.9).

STILL WORK TO DO!!!

A way to quantify the degree of spatial correlation we shall define 'correlation parameter':

$$K^\lambda = \frac{C_{si}^\lambda}{\sqrt{C_{ss}^\lambda C_{ii}^\lambda}} \quad (2.12)$$

calculated for each direction ( $\lambda = x, y$ ) from the covariance matrix  $C^\lambda$  with elements  $C_{kj}^\lambda = \langle q_k^\lambda q_j^\lambda \rangle - \langle q_k^\lambda \rangle \langle q_j^\lambda \rangle$ .

### 2.1.3 Tunable Spatial Correlation SPDC source light

It is clear that both 2.7 and 2.8 depend on  $w_p$ , the pump waist. If we change this parameter and keep the rest of the parameters constant, the term in the exponential function  $[-w_p^2(\Delta_0^2 + \Delta_1^2)/4]$  will variate, making changes in the shape of the original mode function. As it was mentioned here before and in [11], the mode function contains all the informations about the correlations of the generated down converted photons. Hence changing the pump waist  $w_p$  will change the correlations of the generated pair of photons.

## 2.2 Imaging

Assuming we have an object that have its own light or its externally illuminated, imaging means collecting that light that is emitted from the object. Each point of the surface of the object will emit spherical waves to all possible directions, being this said, What is the probability to have a spherical wave collapsing into a point or small spot? Obviously, the chance is practically zero unless an imaging system is applied.

The concept of optical imaging was well developed in classical optics and the Figure 2.4 schematically illustrates a standar imaging setup. In this setup an object is illuminated by a radiation source, an imaging lens is used to focus the scattered and reflected light from the object onto an image plane which is defined by the “Gaussian thin lens equation”[12]:

$$\frac{1}{S_o} + \frac{1}{S_i} = \frac{1}{f} \quad (2.13)$$

where  $S_o$  is the distance between the object and the imaging lens,  $S_i$  the distance between the imaging lens and the image plane, and  $f$  the focal lenght of the imaging lens. This equation defines a point-to-point relationship between the object plane and the image plane: any radiation starting from a point on the object will colapse at a certain point at the image plane.

This one-to-one correspondence in the image-forming relationship between the object and the image planes produces a perfect image. The observed image can be magnified or demagnified, for example, in the Figure 2.4 the original object is a tree, and it is demagnified at the image plane. This depends

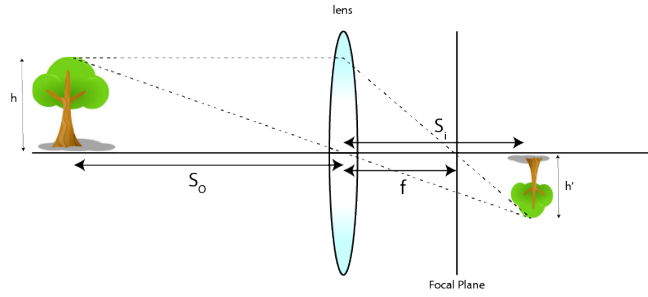


FIGURE 2.4: Optical imaging: a lens produces an image on an object at  $S_i$ . This distance is defined by the Gaussian thin-lens equation

on which optical system are we using, what kind on lenses are involved and the distance between object and them.

### 2.2.1 Standar Imaging

The observed image is a reproduction of the illuminated object, mathematically corresponding to a convolution between the object distribution function  $|T(\vec{\rho}_o)|^2$  (aperture function) and a  $\delta$ -function, which is present for the perfect point-to-point correspondence [13]:

$$\langle I(\vec{\rho}_i) \rangle = \int_{obj} d\vec{\rho}_o |T(\vec{\rho}_o)|^2 \delta(\vec{\rho}_o + \frac{\vec{\rho}_i}{m}) \quad (2.14)$$

where  $\langle I(\vec{\rho}_i) \rangle$  is the mean intensity at the image plane,  $\vec{\rho}_o$  and  $\vec{\rho}_i$  are 2-D vectors of the transverse coordinates,  $\vec{\rho}_n = (x_n, y_n)$ , in the object and image planes, respectively, and  $m = s_i/s_o$  is the image magnification factor.

In reality, we are limited by the finite size of the optical system, we may never obtain a perfect image. The incomplete constructive-destructive interference turns the point-to-point correspondence into a point-to-'spot' relationship. The  $\delta$ -function in the convolution of equation 2.14 will be replaced by a point-to-'spot' image-forming function, or a point-spread function,

$$\langle I(\vec{\rho}_i) \rangle = \int_{obj} d\vec{\rho}_o |T(\vec{\rho}_o)|^2 \text{somb}^2[\frac{\pi D}{\lambda S_o} |\vec{\rho}_o + \frac{\vec{\rho}_i}{m}|] \quad (2.15)$$

where the sombrero-like point-spread function is defined as  $\text{somb}(x) \equiv 2J_1(x)/x$ , with  $J_1(x)$  the first-order Bessel function, and  $D$  the diameter of the imaging lens. It is clear from equation 2.15 that the finite size of the spot in the point-to-'spot' correspondence is determined by some parameters, if we want to have a almost-perfect correspondence we would like to not place

the lens to far away from the object,  $S_o$ . A big imaging lens, and with "big" I refer to its diameter,  $D$ . Imaging usually uses a wide variety of photons with different frequencies<sup>1</sup> if we were able to filter the light that illuminates the object, we would like to choose a short wavelength  $\lambda$ .

This finite size of the spot in the point-to-"spot" relationship we described before, is what is called spatial resolution. A higher spatial resolution of the image is achieved by the conditions described before. Another daily situation in which we are forming images, is when we take a picture. Cameras manufacturers play with these parameters to achieve a high spatial resolution, a spot-to-pixel correspondence. For further informations about this "real life" situation check the ??.

## 2.2.2 Two-photon Imaging

Two-photon imaging consists after all, in reconstructing an image of an object. But in this case we use two detectors located in different paths of the light. By using the detections of them separately we get a constant signal, with no information about the object, Figure 2.5. But if instead we use the signal of both of them, counting coincidences, we can reconstruct the double slit in Figure 2.5.

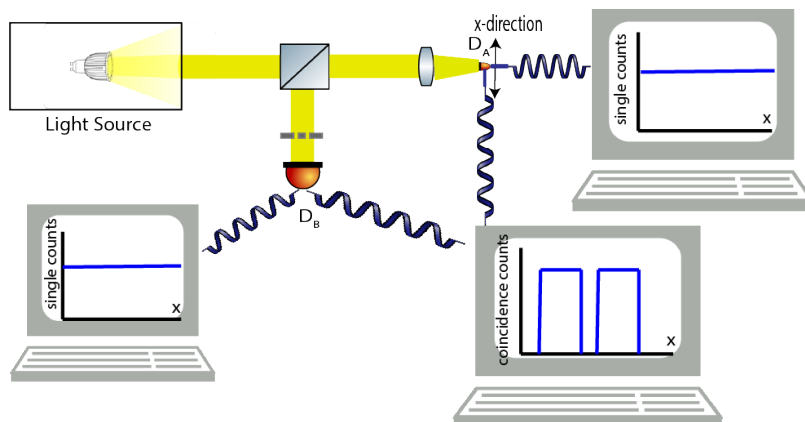


FIGURE 2.5: Simple schematic for the Two-photon Imaging

In order to reconstruct the image of the double slit, we have to introduce some kind of spatial dependence, the object, in this case the double slit, is distributed along a transverse direction of the light propagation. But what we

<sup>1</sup> Imaging forming, as the process done by our eyes and brain uses a big range of photon frequencies, this range is called the *visible spectrum* ( $\sim 390 - 700\text{nm}$ ), the images produced by our eyes are formed just from photons that are at these frequencies, the rest of the photons are ignored by our eyes

have learnt is that scanning along the x-direction (assuming that light propagates along the z-direction), in the path that have no interaction with the object  $D_A$ , and collecting all the light that interacts with the object  $D_B$ , gathering no spatial information. We reconstruct the double slit in the coincidences counts, every time we have a photon detected going through the double slit, and a photon at a certain position  $x_i$ , we graph coincidences vs  $x_i$  and we get the image of the double slit, Figure 2.5.

The standard imaging used the photons at the image plane, to form the image. In other words it measures one photon per spot at the image plane. For the two-photon imaging, in certain aspects the behaviour is similar as that of the classical. They both exhibit a similar point-to-point imaging-forming function, except the two-photon image is only reproducible in the joint-detection between two independent photodetectors, and the point-to-point imaging-forming function is in the form of second-order correlation,

$$R_{BA}(\vec{\rho}_A) = \int_{obj} d\vec{\rho}_B |T(\vec{\rho}_B)|^2 G^{(2)}(\vec{\rho}_B, \vec{\rho}_A) \quad (2.16)$$

where  $R_{BA}(\vec{\rho}_B)$  is the joint-detection counting rate between photodetectors  $D_B$  and  $D_A$ .  $G^{(2)}(\vec{\rho}_B, \vec{\rho}_A)$  is a nontrivial point-to-point second-order correlation function, corresponding to the probability of observing a joint photo-detection event at the coordinates  $\vec{\rho}_B$  and  $\vec{\rho}_A$ . The physics behind  $G^{(2)}(\vec{\rho}_B, \vec{\rho}_A)$  is what changes between the different kinds of two-photon imaging.

This second-order correlation function is defined as[13]:

$$G^{(2)}(\vec{\rho}_B, \vec{\rho}_A) = \frac{\langle E^*(\vec{\rho}_B)E^*(\vec{\rho}_A)E(\vec{\rho}_B)E(\vec{\rho}_A) \rangle}{\langle |E(\vec{\rho}_B)|^2 \rangle \langle |E(\vec{\rho}_A)|^2 \rangle} \quad (2.17)$$

### 2.2.2.1 Two-photon Imaging using entangled photon

In the previous section we introduced the notion of two-photon imaging, but we didn't care much about the nature of the source light. For this case we will use entangled photons as the source light, we will separate the pair of entangled photons by means of a polarization beamsplitter. The first two-photon imaging experiment was demonstrated by Pittman in 1995[1]. The schematic setup of the experiment is shown in the Figure 2.6.

A continuous wave (CW) laser is used to pump a type-II nonlinear crystal to produce pairs of entangled photons. These pairs of orthogonally polarized signal and idler photons are the product of the nonlinear optical process of

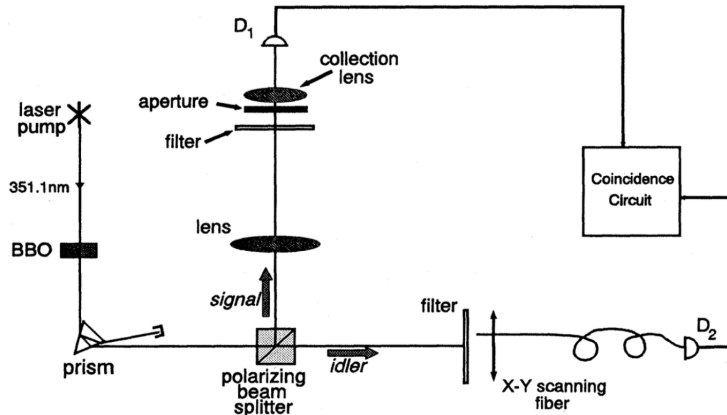


FIGURE 2.6: Schematic of the first "two-photon imaging" experimental setup, used by Pittman[1]

spontaneous parametric down-conversion (SPDC). The pair emerges from the crystal collinearly<sup>2</sup>, it is separated by a dispersion prism, and then the signal and idler are sent in different directions by a polarization beam slitting Glan-Thompson prism.

The reflected signal beam passes through a convex lens with a 400mm focal length and illuminates an aperture<sup>3</sup>. Before the aperture is placed a filter, this is a bandwidth spectral filters centered at the wavelength 702.2nm. Behind the aperture is the detector package  $D_1$ .

The transmitted idler beam is met by detector package  $D_2$ . The input tip of the fiber is scanned in the transverse plane. The counts are sent to a coincidence counting circuit with a 1.8ns acceptance window. An important fact of this experiment is the use of a lens(collection lens) in the signal beam that establishes an image plane with the definitive point-by-point correspondence object(mask) plane.

### 2.2.2.2 Propagation of light through 2-f system

In order to treat this problem in a more general way it, we need to know the state of the biphoton at the output of the crystal:

$$\tilde{\Phi}_c(q_c, q_c) = Ne^{-\frac{1}{2}x^T Ax + ib^T x} \quad (2.18)$$

<sup>2</sup>The pairs emerge from the crystal nearly collinearly, with  $\omega_s \simeq \omega_i \simeq \omega_p/2$ . where the subscript letter stands for signal, idler and pump respectively

<sup>3</sup>The aperture consisted of the letters UMBC, University of Maryland Baltimore County.

Then from this result we can use the fresnel propagation theory to analytically model the biphoton propagation in any arbitrary Two-photon Imaging/Lensless Two-photon Imaging setup. This propagation is done by determining the Green function of the optical path by which the beams will travel.

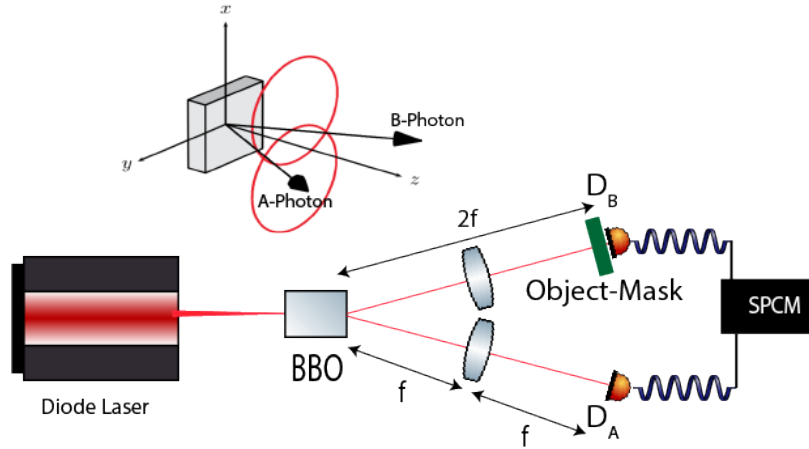


FIGURE 2.7: Simple schematic for a Two-photon Imaging using entangled photons and a 2-f system

Since both path A and B have an identical 2-f system, we are at the called Fourier plane. It is well known that when the light goes through this system suffers a Fourier transform[13]. It means that if we treated the photons as an ensemble of many oscillating in coherent modes, there is a relation between the initial  $q_c$  initial transverse momentum at the crystal, and the  $r_f$  final position of the photons. This relation is:

$$q_{initial} = \frac{2\pi}{\lambda f} r_{final} \quad (2.19)$$

where  $q_{initial}$  is the transverse momentum of the light before the 2-f system,  $r_{final}$  is the position of photon after going through the lens and traveling a 2-f distance.  $f$  stands for the focal length of the lenses used and  $\lambda$  for the frequency of the coherent mode.

The Green function that propagates light with transverse momentum  $q$  from the source, to the Fourier plane located at a position  $r_f$  is[14]:

$$G(q, r_f) = \int d^2 r_l \int d^2 r_c h(r_f - r_l, f) L_f(r_l) h(r_l - r_c, f) e^{iq \cdot r_c} \quad (2.20)$$

with  $r_c$  and  $r_l$  denoting the transverse position vectors in the plane of the crystal and the lens respectively.  $h(r_f - r_l, f)$  and  $h(r_l - r_c, f)$  are the Fresnel

propagators<sup>4</sup> that propagates light from  $r_l$  to  $r_f$  and  $L_f(r) = \Psi(r, -f)$  is the thin-lens transfer function associated to a lens[14].

Taking advantage of the 2-f system as a Fourier transform to reduce the amount of calculations , using the relation 2.19, and after solving the integrals over  $r_l$  and  $r_c$ , equation 2.20 can be written as:

$$G(q, r_f) = Ce^{\frac{i\pi}{\lambda f}r_f^2}e^{\frac{i\lambda f}{4\pi}q^2}\delta\left(q - \frac{2\pi}{\lambda f}r_f\right) \quad (2.21)$$

where C is a complex constant and  $\lambda$  is the wavelenght of the used light. Then we can finally propagate biphoton function in terms of transverse momenta. Where  $\Phi_1(q_B, q_A)$  is the biphoton after traveling through two arbitrary optical paths, it can be expressed in terms of the corresponding Green functions and the initial biphoton function, equation 2.18,  $\tilde{\Phi}_c(q_c, q_c)$  as:

$$\Phi_1(q_B, q_A) = G_B(q_B, r_B)G_A(q_A, r_A)\tilde{\Phi}_c(q_c, q_c) \quad (2.22)$$

$$\Phi_1(r_B, r_A) = \int d^2q_B d^2q_A \Phi_1(q_B, q_A) \quad (2.23)$$

where  $r_B$  and  $r_A$  denotes the photon position in the transverse plane at a 2-f distance from the crystal, the subscript stand for the different path followed by light, Figure 2.7. The  $G_B(q_B, r_B)$  and  $G_A(q_A, r_A)$  are the green functions for each path, defined as in equation 2.21, they are:

$$G_B(q_B, r_B) = G(q_B, r_B) \times T(r_B) \quad (2.24)$$

$$G_A(q_A, r_A) = G(q_A, r_A) \quad (2.25)$$

Where  $T(r_B)$  is the transfer function of the object, which is only present at the B path, Figure 2.7. Gathering all the previous results we can obtain  $\Phi_1(r_B, r_A)$ . This is done by replacing Eq. 2.24 and 2.25 into Eq. 2.22, then evaluating the integrals over the transverse momentums, Eq. 2.23, we obtain:

$$\Phi_1(r_B, r_A) = C^2 T(r_B) \Phi\left(\frac{2\pi}{\lambda f}r_B, \frac{2\pi}{\lambda f}r_A\right) \quad (2.26)$$

This function describes the biphoton at the planes of the object and the scanning detector. It shows that the biphoton at the 2F plane as a function of  $r_B$  and  $r_A$ . If we take a closer look, this result enable us to compute the biphoton at the 2-F plane by using Eq 2.9 without the need to actually calculate its propagation, just by evaluating it with the Fourier relationship, 2.19. This is

---

<sup>4</sup>Fresnel Propagator:  $h(r, z) = \left(-\frac{i}{\lambda z}\right)e^{(i\frac{2\pi z}{\lambda})}\Psi(r, z)$  with  $\Psi(r, z) = e^{(i\frac{\pi}{\lambda z})r^2}$ .

specially usefull when we try to simulate this on a computer, the amount of calculations is significantly reduced by this fact.

As described at the beginning of this Section 2.2.2, we lose all the spatial information about the photon that interacts with the Object, and this is done by placing a bucket detector that gathers all light and send it to a multimode optic fiber, without saving any information about the position of the photons in this path  $B$ . From the mathematical point of view, the bucket detector is modeled as:  $\Phi_1(r_A) = C^2 \int d^2r_B T(r_B) \Phi(\frac{2\pi}{\lambda_f} r_B, \frac{2\pi}{\lambda_f} r_A)$ . Using the fact that the coincidence counts that will be measured by the Detectors will be proportional to the magnitude square of the resulting biphoton function  $\Phi_1(r_A)$ [13].

$$S(r_A) \propto \left| \int d^2r_B T(r_B) \Phi\left(\frac{2\pi}{\lambda_f} r_B, \frac{2\pi}{\lambda_f} r_A\right) \right|^2 \quad (2.27)$$

Where  $S(r_A)$  is the function that describes de coincidences counts between de detectors  $D_B$  and  $D_A$  in Figure 2.7.  $S(r_A)$  is a function of the spatial positions,  $(x_A, y_A)$  of the detection plane at  $D_A$ . This function  $S(r_A)$  have the expected behaviour described by  $R_{BA}(\vec{\rho}_A)$  in Eq. 2.16, where the second-order correlation function in this case is  $\Phi(\frac{2\pi}{\lambda_f} r_B, \frac{2\pi}{\lambda_f} r_A)$ , as we said, the function containing all the informations about the correlations between the pair of down-converted photons. Moreover, Equation 2.27 indicates that the form of  $\Phi(q_B, q_A)$  determines if  $T(r_B)$  can be recovered in the coincidence count. Additionally, the type of spatial correlation in  $\Phi(q_B, q_A)$  defines the orientation of the image obtained.

### 2.2.2.3 Two-photon Imaging Using Chaotic Sources

In principle the term "thermal radiation" should refer only to radiation coming from a blackbody in thermal equilibrium at some temperature T. But with this realisation of thermal radiation we have to face some characteristics of true thermal fields. Thermal radiation is also referred as chaotic light, which have extreme short coherence time. This is because a thermal source contains a large number of independent sub-sources, such as the trillions of atoms or molecules. These atomic transitions that can be identical or different act like sub-sources, that emit light into independently and randomly.

The source light in Figure 2.8 is the one developed by Martinssen and Spiller[15] which is the most commonly used among the pseudothermal fields. A coherent laser radiation is focused on a rotating ground glass disk, the scattered radiation is chaotic with a Gaussian spectrum. After this, a nonpolarizing beam splitter (BS) splits the radiation in two distinct optical pths, In

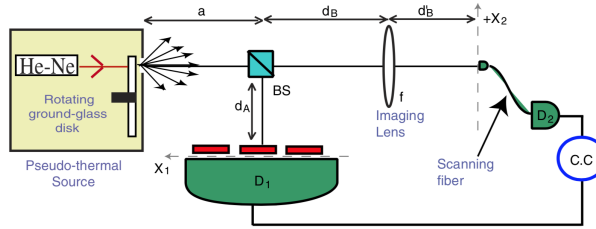


FIGURE 2.8: Experimental setup for the Two-photon imaging using thermal light, taken from [2]

the reflected arm an object, with transmission function  $T(r_1)$ , is placed ar a distance  $d_A$  from the BS and a bucket detector ( $D_1$ ) is just behind the object. In the transmitted arm an imaging lens, with focal lenght  $f$ , is placed at a distance  $d_B$  from the BS, and a multimode optical fiber ( $D_2$ ) scans the transverse plane at a distance  $d'_B$  from the lens. The output pulses from the two single photon counters are sent to an electronic coincidence circuit to measure the rate of coincidence counts.

Once again we expect the joint-detection counting rate between photodetectors  $D_1$  and  $D_2$  to behave like the one described in Eq. 2.16. But thos rate this coincidence counts is governed by the second-order Glauber correlation function [16]:

$$G^{(2)}(\vec{r}_1; \vec{r}_2) \equiv \langle E_1^{(-)}(\vec{r}_1) E_2^{(-)}(\vec{r}_2) \times E_2^{(+)}(\vec{r}_2) E_1^{(+)}(\vec{r}_1) \rangle \quad (2.28)$$

where the  $E^{(-)}$  and  $E^{(+)}$  are the negative-frequency and the positive-frequency field operators describing the detection events at the locations  $\vec{r}_1$  and  $\vec{r}_2$ . The transverse second-order correlation correlation function for a thermal source is given by [2]:

$$G_{\text{thermal}}^{(2)}(\vec{r}_1; \vec{r}_2) \propto \sum_{\vec{q}} |g_1(\vec{q}, \vec{r}_1)|^2 \sum_{\vec{q}'} |g_2(\vec{q}', \vec{r}_2)|^2 + |\sum_{\vec{q}} g_1^*(\vec{q}, \vec{r}_1) g_2(\vec{q}, \vec{r}_2)|^2 \quad (2.29)$$

where  $\vec{r}_i$  is the transverse position of the detector  $D_i$ ,  $\vec{q}$  and  $\vec{q}'$  are the transverse components of the momentum vectors, and  $g_i(\vec{q}, \vec{r}_i)$  is the Green's function associated with the propagations of the field with transverse momentum  $\vec{q}$  from the source, to the position  $\vec{r}_i$  at the detection plane defined by the detector  $D_i$ .  $g_i(\vec{q}, \vec{r}_i)$  is defined in a similar way as in Eq. 2.20.

It is important to note that there are two main differences with respect to the SPDC case: First the presence of a background noise (first term of Eq. 2.29), which does not exist for SPDC. Second, the possibility of writing the

second term of Eq. 2.29 as a product of the first order correlation functions,  $G_{12}^{(1)}G_{21}^{(1)}$ , while there is no way to write the biphoton produced by the SPDC as a product of other correlations. Also this term  $|\sum_{\vec{q}} g_1^*(\vec{q}, \vec{r}_1)g_2(\vec{q}, \vec{r}_2)|^2$  Is the interference of intensities of a incoherent statistical assemble of randomly distributed photons.

Following the proces done in [2], it can be shown that for any values of distances  $d_A$ ,  $d_B$  and  $d'_B$  which obey the equation:

$$\frac{1}{d_B - d_A} + \frac{1}{d'_B} = \frac{1}{f} \quad (2.30)$$

which clearly has the form on a thin-lens equation, defining a point-to-point correspondence between imaging and object plane. Then Eq. 2.29 can be simplified as:

$$G_{tot}^{(2)}(\vec{r}_2) \propto N + |T\left(\frac{d_A - d_B}{d'_B}\vec{r}_2\right)|^2 \quad (2.31)$$

where  $T\left(\frac{d_A - d_B}{d'_B}\vec{r}_2\right)$  is the object transmission function ( $T(\vec{r}_1)$ ) reproduced on the  $D_2$  plane. Thanks to this result we can conclude that a thermal source allows reproducing in coincidence measurements the two-photon image of an object, similarly to the SPDC case, except for a constant background noise, where  $N$  is proportional to it.

It is possible to establish an analogy between classical optics and entangled two-photon optics: the two-photon probability amplitude plays in entangled two-photon processes the same role that the complex amplitude of the electric field plays in classical optics [2].

# Chapter 3

## Experimental Setup

### 3.1 SPDC Setup

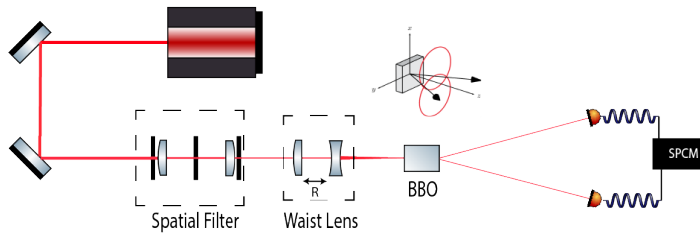


FIGURE 3.1: Experimental Setup for the SPDC light Source

#### 3.1.1 Diode Laser

The light source used in this experiment is a Diode Laser that delivers a continuous wave(CW) at  $\lambda = 406,101\text{nm}$  and  $\Delta\lambda = 4\text{nm}$ . The laser model No. DL 405-200 delivers light at 200 mW with a beam diameter of 1.5 mm and a beam Divergence 1.2 mrad. IN HERE I MAY TALK ABOU THE M FACTOR, QUALITY PARAMETER OF GAUSIAN BEAMS  $M^2$  Power 200mW

#### 3.1.2 Mirror

further details to be asked,

#### 3.1.3 Spatial Filter

A laser beam can be characterized by measuring its spatial intensity profile at points perpendicular to its direction of propagation. The spatial intensity profile is the variation of intensity as a function of distance from the center of the beam, in a plane perpendicular to its direction of propagation. In



FIGURE 3.2: Image of the Diode Laser and it's control module,  
Taken from [3]



FIGURE 3.3: Mirror and the cavity mount

the Figure 3.4(top part) we see the input gaussian beam and how its intensity fluctuates around the x axis. The output desired beam after going

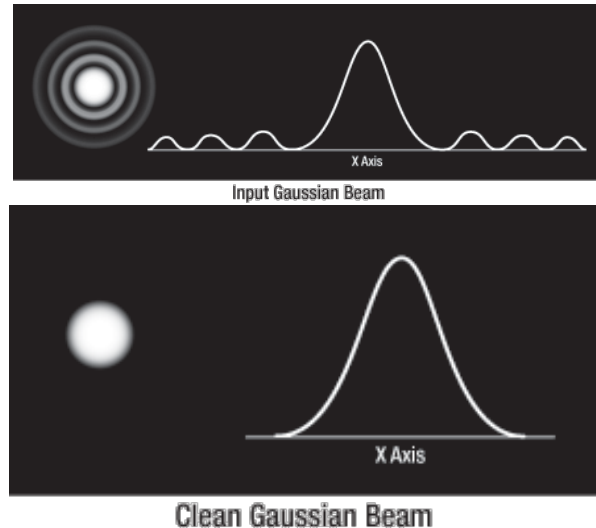


FIGURE 3.4: The spatial intensity profile before and after the spatial filtering process , Taken from [4]

through the spatial filter is shown at the bottom of the Figure 3.4. The simplest arrangement to achieve this output spatial intensity profile is show in the Figure 3.5, where at the end we have a beam which intensity strength falls off transversely following a bell-shaped curve that's symmetrical around the central axis. Taking a closer look at the Figure 3.4 (top part) we may recognise

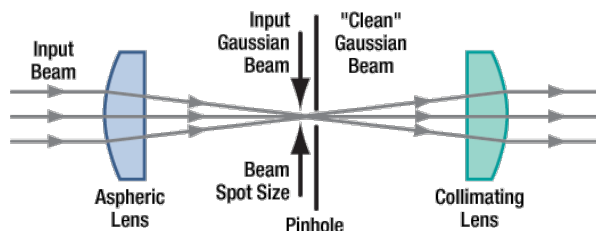


FIGURE 3.5: Basic elements of a Spatial Filter. In our experiment we use a Aspheric Lens of  $f = 30\text{mm}$ (LA1805-A), a pin-hole of  $50\mu\text{m}$  and a collimating lens of  $f = 60\text{mm}$ (LA1134-A).  
Taken from [4]

a diffraction pattern, but when we measure this spatial profile directly from the diode laser, we find out that it doesn't follow that behaviour, on the contrary it follows a more random spatial profile. This ramdom spatial profile is a result of the randomnes in the quantum emissions and absorptions that are happening at the exited atoms at the diode laser[12].

In order to have this spatial intensity profile at the input of my lens arrangement, Figure 3.5, we put a circular aperture with the help of a pair of irises, Figure 3.6, before the  $f = 30.0\text{mm}$  lens and after the  $f = 60.0\text{mm}$  lens.



FIGURE 3.6: This helps to form circular apertures of variable radius

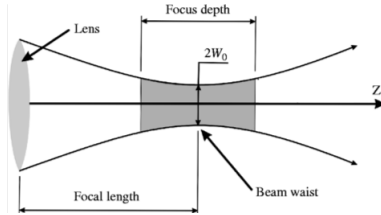


FIGURE 3.7: Lens' effect on a Gaussian beam

### 3.1.4 Waist Lens

A Gaussian beam hits a lens.... To control the pump waist we can put a lens in the propagation direction with certain focal length  $f$ . This lens will define a zone around the distance  $f$  called *Focus depth*[12] , where in the middle we find the narrowest point of the beam, Figure 3.7. The radius of this zone is:

$$W_0 = \frac{\lambda f}{\pi W_B} \quad (3.1)$$

Where  $W_B$  is the initial waist beam.

If we want to focus the beam at a fixed distance  $F$ , using this method to control the pump waist is not practical. Every different lens we would use will make this waist  $W_0$  at a different distances  $f$ . It is necessary to find a *Waist lens* that make us a waist  $W_0$  at a transverse plane located in a fixed position  $F$  from the *Waist Lens*. This special lens consists in an arrangement of two lenses, a positive and negative one respectively, separated a distance  $d_0$  from each other. SOURCE WHERE THEY EXPLAIN HOW TO USE A POSITIVE AND NEGATIVE ASK OMAR!!!

### 3.1.5 BBO(Beta Barium Borate) Crystal

the power of the pump is  $60mW$  The nonlinear optical media used in this experiment is a BBO(Beta Barium Borate) crystal, this crystal is  $5x5x4mm$ . BBO ( $(\beta\text{-BaB}_2\text{O}_4)$ ) The crystal is mounted in such way that the input and output plane are fixed, Figure 3.8.

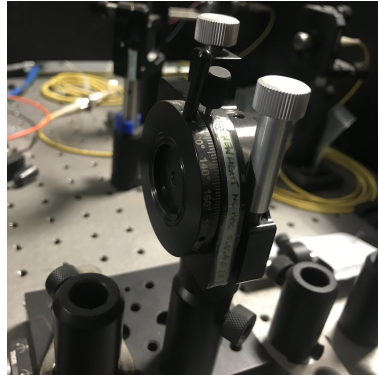


FIGURE 3.8: Actual BBO crystal used in experiment

## 3.2 Spatial Correlations Measurement Setup

From this point we will talk about a pair of entangled photon pairs, that will come from the output plane of the BBO crystal, for historical reasons we will label this pairs as *signal* and *idler*.

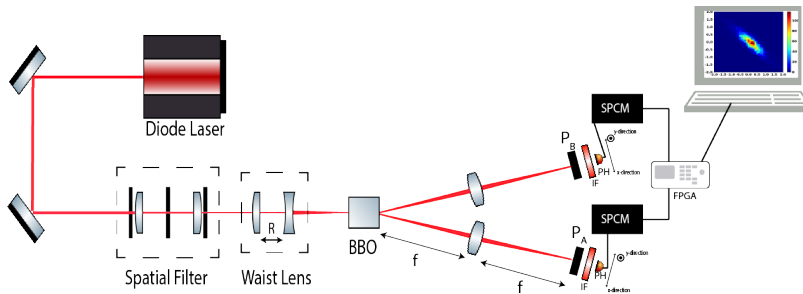


FIGURE 3.9: Experimental Setup for Obtaining the spatial correlations of a pair of down-converted photons

### 3.2.1 Lens (Fourier Plane)

To define the  $2f$  system we use a lens(LA1708) of  $f = 200.0\text{mm}$  in front of each *signal* and *idler*. This lens is placed at a distance  $f$  from the output plane.

### 3.2.2 Polariser

In order to be able to filter certain polarisation direction we used a pair of Polarisers(WP25M-UB), which consist in a circular surface than only transmit the light that comes in a specific direction. other directions are reflected

### 3.2.3 Interferometer Filter

In this situation we are interested in the correlations in the space variables, hence we would like to filter all this time variables. To do this filtering we used a spectral filter(FB810-10) that only transmits the light that comes with  $\lambda = 810 \pm 2nm$ .

### 3.2.4 Pin Hole(Arduino)

MORE DETAILS, HOW MANY ARDUINOS, coupling lens reference ETC ...

### 3.2.5 Single Photon Counting Module(SPCM)

To detect photons we a self-contained module that detects single photons of light over the  $400nm$  to  $1069nm$  wavelength range. The module used (SPCM-AQRH-13) uses a unique silicon avalanche photodiode (SLiK) with a detection efficiency of more than 65%[17]. Light is transmitted through a optic fiber from the pin hole detector to the SPCM. The result signal coming from the SPCM are pulses that represents one photon detections.



FIGURE 3.10: Single Photon Counting Module

### 3.2.6 Field-programmable gate array(FPGA)

Both *signal* and *idler* pulses from the respective SPCM goes to the same FPGA(ZestSC1). This Field-programmable gate array is programmed to count the photon coincidences, this means that the FPGA is fast enough to detect and separate pulses from photons that are time-separated.

### 3.2.7 Computer(Data Analysis)

labview is used to control the detection module, where it delivers a list of the detection, graph are made with any program language able to handle the data.

## 3.3 Two-Photon Imaging Setup

For the Two-photon imaging process we no longer have spatial information about the *signal* photon after it interacts with the mask

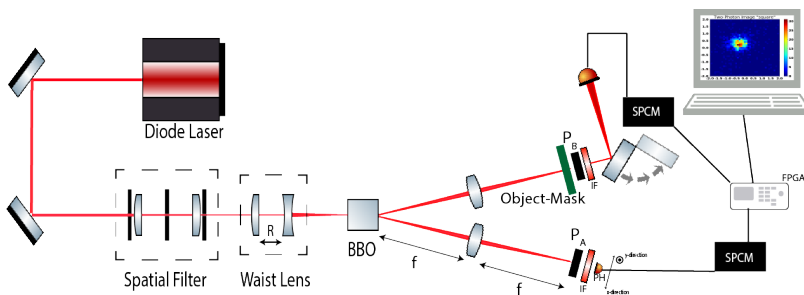


FIGURE 3.11: Experimental Setup for the Two-photon Imaging

### 3.3.1 Mask

This is an obstruction that is placed in the *signal* path with certain shape, it could be a mask with the shape of a letter or any other geometry. This is the object of which we want to construct an image.

### 3.3.2 Folding Mirror

In order to change the path followed by the *signal* photon, we use a Folding mirror, Figure 3.12. This mirror can be in the *signal* path or not.

### 3.3.3 Bucket Detector

This detector consists in a coupling lens that collects all the light that goes through the mask. In contrast to the other detections made in this experiment, the Bucket detector loses track of any spatial information of the *signal* photon. Another big difference is that this Bucket detector uses a multimode optic fiber to take the light to the SPCM.



FIGURE 3.12: Foldind Mirror, it is in the position for measuring the correlations

# Chapter 4

## Results

### 4.1 Achiiving a Gaussian Beam

here comes de data od the new laser

### 4.2 Finding The Correlated Photons

SPDC nocolinear type II

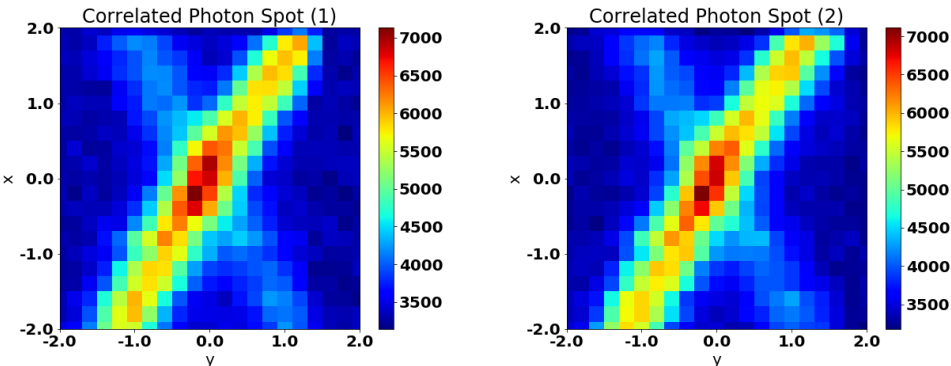


FIGURE 4.1: We are moving the translational stage, to locate the spot where the correlated photon are, for this try me moved the  $y$  direction

### 4.3 Experimental Correlations

Info taken before me

### 4.3.1 $w_p = ?$

## 4.4 Mask Alignment

We want that most of the correlated photon hits the mask

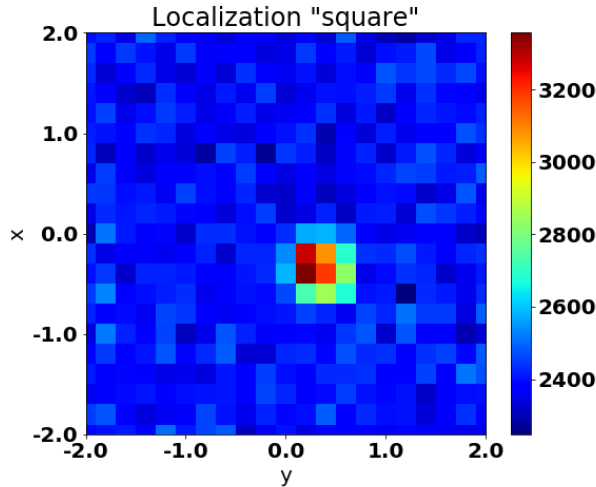


FIGURE 4.2: Localization of the mask with an square

changing to the mask with an L

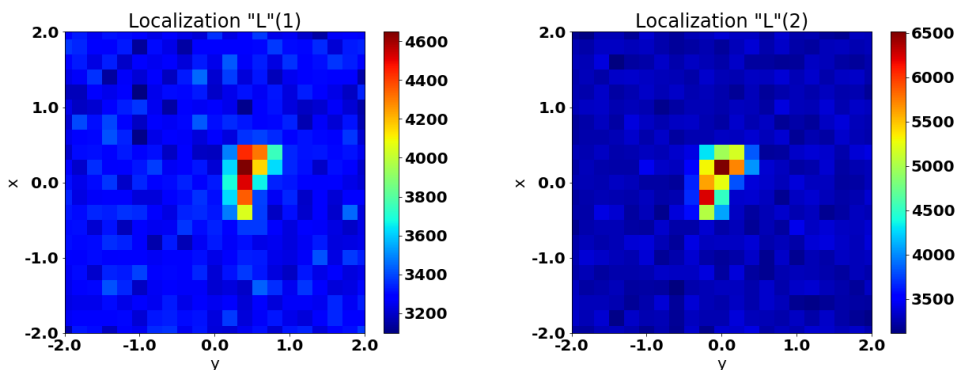


FIGURE 4.3: Moving the L Mask in order to put it in the most central spot

Long Exposure

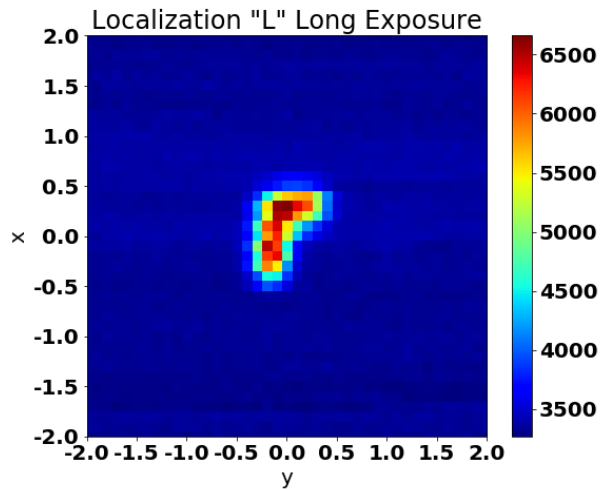


FIGURE 4.4: Long exposure of the definitive localization of the mask, in this try we leave the detector in each place for 30 seconds, we also make the steps of the detector smaller,  $0.1\text{mm}$

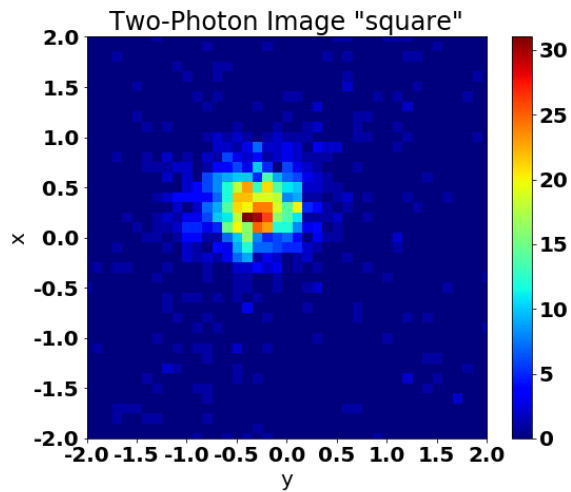


FIGURE 4.5: Localization of the mask with an square

## 4.5 Two-Photon Images

### 4.5.1 mask1

### 4.5.2 mask2

### 4.5.3 mask3

## Chapter 5

# Discussions and Conclusion

In summary, we may conclude that ghost imaging is the result of quantum interference. Either type-one or type-two, ghost imaging is characterized by a non-factorizable point-to-point image-forming correlation which is caused by constructive-destructive interferences involving the nonlocal superposition of two-photon amplitudes, a nonclassical entity corresponding to different yet indistinguishable alternative ways of producing a joint photo-detection event. The interference happens within a pair of photons and at two spatially separated coordinates. The multi-photon interference nature of ghost imaging determines its peculiar features: (1) it is non-local; (2) its imaging resolution differs from that of classical; and (3) the type-two ghost image is turbulence-free. Taking advantage of its quantum interference nature, a ghost imaging system may turn a local “bucket” sensor into a nonlocal imaging camera with classically unachievable imaging resolution. For instance, using the Sun as light source for type-two ghost imaging, we may achieve an imaging spatial resolution equivalent to that of a classical imaging system with a lens of 92-meter diameter when taking pictures at 10 kilometers.<sup>10</sup> Furthermore, any phase disturbance in the optical path has no influence on the ghost image. To achieve these features the realization of multi-photon interference is necessary[9].

# Bibliography

- [1] T B. Pittman, Yanhua Shih, D V. Strekalov, and Alexander Sergienko. Optical imaging by means of two-photon quantum entanglement. *Physical review. A*, 52:R3429–R3432, 12 1995.
- [2] Alejandra Valencia, Giuliano Scarelli, Milena D’Angelo, and Yanhua Shih. Two-photon imaging with thermal light. *Phys. Rev. Lett.*, 94:063601, Feb 2005.
- [3] Crystal laser. <http://www.crystalaser.com>. Accessed: 2018-03-09.
- [4] Thorlabs, inc. <https://www.thorlabs.com/index.cfm>. Accessed: 2018-03-09.
- [5] Jefferson Flórez, Omar Calderón, Alejandra Valencia, and Clara I. Osorio. Correlation control for pure and efficiently generated heralded single photons. *Phys. Rev. A*, 91:013819, Jan 2015.
- [6] M. D’Angelo and Y. Shih. Can quantum imaging be classically simulated? *eprint arXiv:quant-ph/0302146*, February 2003.
- [7] A. Einstein, B. Podolsky, and N. Rosen. Can quantum-mechanical description of physical reality be considered complete? *Phys. Rev.*, 47:777–780, May 1935.
- [8] Clara I Osorio, Alejandra Valencia, and Juan P Torres. Spatiotemporal correlations in entangled photons generated by spontaneous parametric down conversion. *New Journal of Physics*, 10(11):113012, 2008.
- [9] Jeffrey H. Shapiro and Robert W. Boyd. The physics of ghost imaging. *Quantum Information Processing*, 11(4):949–993, Aug 2012.
- [10] D.S. Shafer and Z. Zhang. *Introductory Statistics*. Saylor.org, 2010.
- [11] Omar Calderón-Losada, Jefferson Flórez, Juan P. Villabona-Monsalve, and Alejandra Valencia. Measuring different types of transverse momentum correlations in the biphoton’s fourier plane. *Opt. Lett.*, 41(6):1165–1168, Mar 2016.

- [12] E. Hecht. *Optics*. Pearson education. Addison-Wesley, 2016.
- [13] Y. Shih. *An Introduction to Quantum Optics: Photon and Biphoton Physics*. Series in Optics and Optoelectronics. Taylor & Francis, 2011.
- [14] Morton H. Rubin. Transverse correlation in optical spontaneous parametric down-conversion. *Phys. Rev. A*, 54:5349–5360, Dec 1996.
- [15] W. Martienssen and E. Spiller. Coherence and fluctuations in light beams. *American Journal of Physics*, 32(12):919–926, 1964.
- [16] Roy J. Glauber. The quantum theory of optical coherence. *Phys. Rev.*, 130:2529–2539, Jun 1963.
- [17] PerkinElmer. *Single Photon Counting Modules – SPCM*, 2010. Rev. 1.